Cell

The Telomere Bouquet Controls the Meiotic Spindle

Kazunori Tomita[1] and Julia Promisel Cooper[1,*]
[1]Telomere Biology Laboratory, Cancer Research UK, London WC2A 3PX, UK
*Correspondence: julie.cooper@cancer.org.uk
DOI 10.1016/j.cell.2007.05.024

SUMMARY

Bouquet formation, in which telomeres gather to a small region of the nuclear membrane in early meiosis, has been observed in diverse eukaryotes, but the function of the bouquet has remained a mystery. Here, we demonstrate that the telomere bouquet plays a crucial role in controlling the behavior of the fission yeast microtubule-organizing center (known as the spindle pole body or SPB) and the meiotic spindle. Using mutations that specifically disrupt the bouquet, we analyze chromosome, SPB, and spindle dynamics throughout meiosis. If the bouquet fails to form, the SPB becomes fragmented at meiosis I, leading to monopolar, multiple, and mislocalized spindles. Correct SPB and spindle behavior require not only the SPB recruitment of telomere proteins but also that the proteins are properly bound to telomeric DNA. This discovery illuminates an unanticipated level of communication between chromosomes and the spindle apparatus that may be widely conserved among eukaryotes.

INTRODUCTION

Sexual reproduction and genetic variation are instigated by the halving and blending of parental genomes that occur during meiosis. To promote reductional nuclear division and homolog recombination, the meiotic cycle differs from the mitotic cycle in key ways. While both have at their core the formation of a spindle that carries chromosomes to opposite ends of the cell in a highly choreographed fashion, the separation of homologs, rather than sisters, at meiosis I entails a different mode of chromosome-spindle interaction. Hence, it is perhaps not surprising that dramatic chromosome movements are an inherent feature of meiotic prophase.

During the early stages of meiosis, all the telomeres in the cell gather at the nuclear envelope, often near the centrosome. This polarized chromosome arrangement has been dubbed the "bouquet," as the collected chromosome ends reminded early 20th century microscopists of the stems of a floral bouquet. The extraordinary conservation of the bouquet throughout eukaryotes suggests that it plays an important role in promoting successful meiosis. As the bouquet stage coincides with the period in which homologous chromosome pairing begins, a reasonable proposal has evolved that by anchoring all chromosome ends within a limited volume, the bouquet functions to facilitate the homology search. Here we extend the view of bouquet function to include a role in setting up a special chromosome-spindle interaction that is crucial for meiotic progression.

The meiotic bouquet of the fission yeast *Schizosaccharomyces pombe* is particularly easy to discern and analyze. The small chromosome number of this organism (three per haploid genome) confers a tight focal appearance to the gathered telomeres, which remain in the bouquet configuration for the entirety of meiotic prophase. Fission yeast grow as haploids, but when they are exposed to conditions of nitrogen starvation, haploids of opposite mating type undergo sexual differentiation, mating, and meiosis, ultimately forming an ascus that contains four haploid spores. These events are accompanied by progressive alterations in nuclear organization: During mitotic interphase, centromeres localize to a single cluster adjacent to the SPB (Funabiki et al., 1993), which is located on the cytoplasmic side of the nuclear membrane (Ding et al., 1997). However, in cells responding to the pheromones that are secreted upon sexual differentiation, the telomeres gather at the SPB. Once these haploids mate to form the zygote, their SPBs fuse, duplicate, and separate from the centromeres, leaving the telomere bouquet as the only connection between chromosomes and the SPB (Chikashige et al., 1994, 1997). This bouquet persists through the subsequent stage in which the nucleus oscillates back and forth through the cytoplasm, creating an elongated nuclear shape that has been dubbed the "horsetail" (Chikashige et al., 1994). This moving nucleus is led by the SPB, which is pulled by cytoplasmic microtubules powered by the meiosis-specific dynein motor (Ding et al., 1998; Miki et al., 2002; Yamamoto et al., 1999). During this horsetail stage, meiotic recombination occurs, having been initiated by Rec12, the fission yeast Spo11 homolog that creates meiotic DNA breaks (De Veaux et al., 1992). Horsetail movement ceases just prior to meiosis I, and the SPB undergoes a poorly defined maturation process, in which its components accumulate and it

divides in two. The resulting SPBs insert into the nuclear membrane, a bipolar intranuclear spindle is generated between them, and the chromosomes undergo the reductional segregation of meiosis I. The telomeres are known to dissociate from the SPB prior to meiosis I (Chikashige et al., 1994). Meiosis II comprises a second round of SPB maturation and spindle formation, followed by equational chromosome segregation.

Several genes involved in bouquet formation have been isolated in *S. pombe*. Fragmentation of the bouquet was first observed in *kms1*Δ cells (Shimanuki et al., 1997). However, this deletion disrupts the SPB itself, while leaving telomeres associated with the dispersed SPB fragments. Bouquet formation itself is disrupted in cells lacking the telomere-binding protein Taz1, its interacting partner Rap1, or the heterochromatin factors Rik1 or Clr4 (Chikashige and Hiraoka, 2001; Cooper et al., 1998; Kanoh and Ishikawa, 2001; Nimmo et al., 1998; Tuzon et al., 2004). Finally, systematic microarray-based screens have recently identified a pair of meiosis-specific proteins, Bqt1 and Bqt2, whose activities are crucial to bouquet formation (Chikashige et al., 2006; Martin-Castellanos et al., 2005; Tang et al., 2006). An elegant series of experiments completed the linkage between telomeric DNA and the SPB by demonstrating the successive interaction of telomere-bound Taz1, Rap1, Bqt1/2, and Sad1, a component of the SPB (Hagan and Yanagida, 1995; Chikashige et al., 2006).

Despite progress in understanding the mechanisms of bouquet formation, its function is still a matter of speculation. The *taz1*Δ strain shows reduced homolog pairing along chromosome arms, although pairing in the centromere region is unaffected (Ding et al., 2004). Furthermore, cells lacking Taz1, Bqt1, or Bqt2 show reduced levels of meiotic recombination (Chikashige et al., 2006; Cooper et al., 1998; Martin-Castellanos et al., 2005; Nimmo et al., 1998). Hence, the idea that the bouquet promotes homologous pairing and meiotic recombination has found qualitative support in accordance with the classic speculation (reviewed in Harper et al., 2004).

However, the extent to which recombination is reduced in bouquet-deficient strains is not entirely consistent with their defects in spore formation. Horsetail-deficient mutants of *S. pombe* (*dhc1*Δ, *ssm4*Δ, *hrs1*(*mcp6*)Δ, and *num1*(*mcp5*)Δ), in which telomeres cluster properly at the SPB but the SPB fails to traverse the zygote, show more severely impaired meiotic recombination than bouquet-defective strains without compromised spore viability (Niccoli et al., 2004; Saito et al., 2006, 2005; Tanaka et al., 2005; Yamamoto et al., 1999; Yamashita and Yamamoto, 2006; and this study). Hence, the bouquet may promote recombination largely by allowing horsetail movement, but it clearly serves other functions that are not dependent on horsetail movement.

These observations stimulated us to explore the phenotypes of cells lacking stable bouquet formation in greater depth. Using fission yeast genetics and live microscopy, we demonstrate that telomere clustering to the SPB is crucial for SPB maturation and proper meiotic spindle formation, highlighting an unexpected level of control of the spindle apparatus by chromosomes.

RESULTS

Characterization of *taz1*Δ*lig4*Δ Meiosis

To investigate the function of the meiotic bouquet, we examined the phenotypes of cells harboring mutations that disrupt bouquet formation. *taz1*$^+$ deletion abolishes the stable association of telomeres with the SPB and yields reduced levels of meiotic recombination along with strikingly aberrant asci whose spores are largely inviable (Cooper et al., 1997, 1998; Nimmo et al., 1998). In principle, the latter defects may stem from the disruption of bouquet formation conferred by *taz1*$^+$ deletion. However, *taz1*Δ zygotes suffer an additional defect, as loss of Taz1 leads to telomere fusions, mediated by the nonhomologous end-joining pathway (NHEJ), during the G1 arrest period that precedes meiosis (Ferreira and Cooper, 2001). To specifically address bouquet function without complications from chromosome end fusions, we deleted the genes encoding participants of the NHEJ pathway (Lig4 or pKu70) in a *taz1*Δ background. *lig4*$^+$ or *pku70*$^+$ deletion prevents *taz1Δ* telomere fusions and partially rescues the defects in ascus formation and spore viability seen in *taz1*Δ meiosis (Tuzon et al., 2004; Figure 1B). Nonetheless, while no meiotic defects are seen in *lig4*Δ single mutants, *taz1*Δ*lig4*Δ meiosis is markedly defective (Figures 1A and 1B).

To characterize the defects in *taz1*Δ*lig4*Δ meiosis, we examined the distribution of DNA and SPB signals in asci in which the SPB component Cut12 (Bridge et al., 1998) is tagged with GFP at its endogenous locus (Figure 1A). Approximately 50% of *taz1*Δ*lig4*Δ asci are normal tetrads in which all spores have equal amounts of DNA and SPB signal (Figures 1Aa and 1B); these spores are largely viable (Figure S1A). However, the remaining *taz1*Δ*lig4*Δ asci are aberrant, having fewer than four spores or four spores of uneven size and shape. The majority of these asci appear to have failed in meiotic progression and have undergone spore formation without completing meiosis (Figures 1Ab–1Ae). We also observe asci in which some DNA is left outside of any spore (Figure 1Af). However, in those asci containing two masses of DNA, the two masses are often equal in DAPI staining intensity (Figure 1Ac), suggesting that when meiosis I does occur, the chromosomes tend to segregate equally. Likewise, in asci containing three masses of DNA, there are usually two masses of equal DAPI staining intensity and a third that is twice as intense, suggesting that meiosis I and II occurred properly in half of the ascus, while meiosis II failed in the other half (Figure 1Ad). Thus, while *lig4*$^+$ deletion partially rescues the profound chromosome segregation defect seen in *taz1*Δ meiosis, meiotic progression in a *taz1*Δ*lig4*Δ background is often impeded and uncoupled from spore formation.

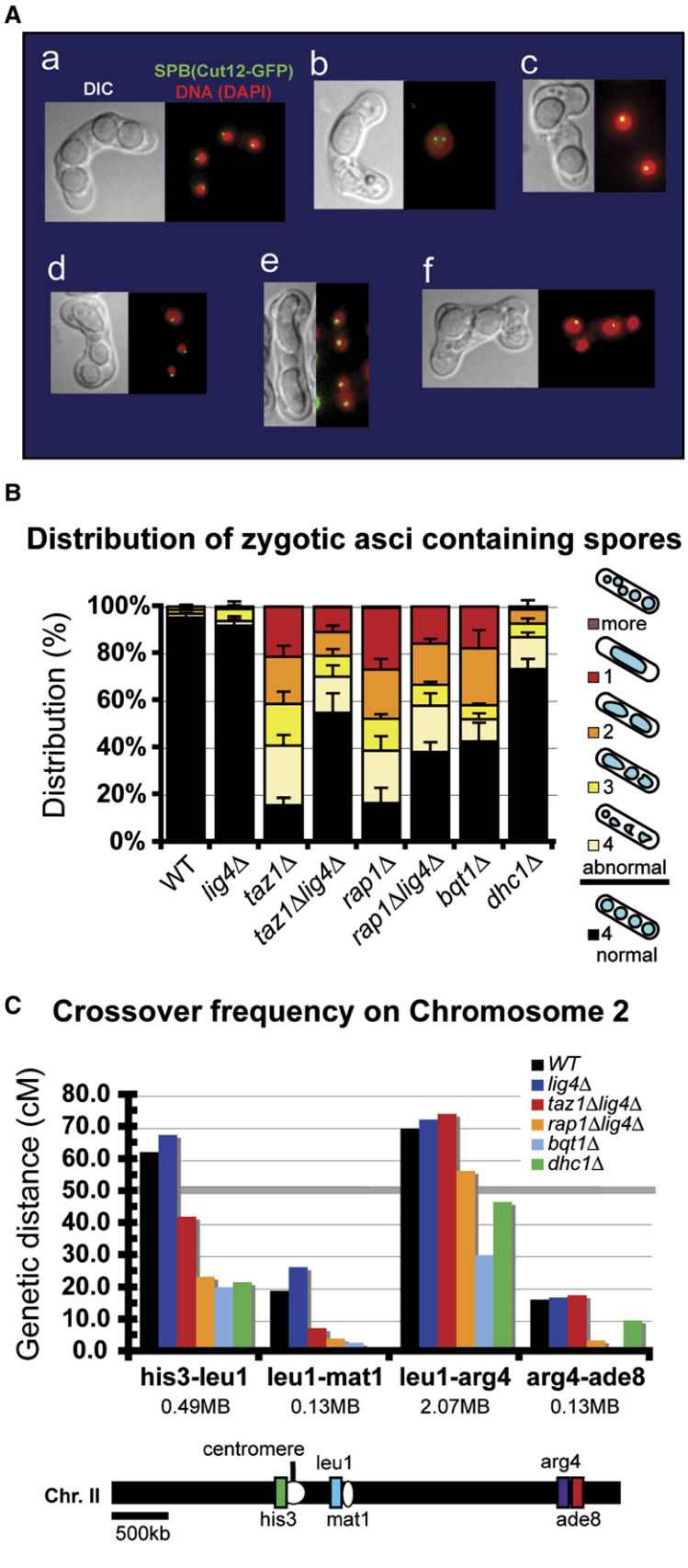

Figure 1. Morphology of Zygotic Asci in Bouquet-Defective Strains

(A) SPB and chromosome distribution in *taz1-Δlig4Δ* asci. Zygotic asci harboring Cut12-GFP were stained with DAPI. (a–f) DIC image (left) and merged GFP and DAPI images (right) are shown. (a) Normal-looking ascus. (b) One-spored ascus. (c) Two-spored ascus. (d) Three-spored ascus. (e) Two-spored ascus whose two spores contain twice their share of DNA and SPBs. (f) Two-spored ascus containing two additional masses of DNA that are not encapsulated.

(B) Distribution of categories of asci. Asci generated from the indicated genotypes in a h^{90} (homothallic) background were scored by light microscopy. Schematic representations of each category are shown to the right of the graph. Two hundred asci per genotype were counted in each experiment. Data represent the average of five experiments. Note that we underestimate the percentage of abnormal asci, as asci that fail to produce spores cannot be distinguished from zygotes and were therefore excluded from our analysis. Error bars indicate standard deviations.

(C) Bouquet-defective meiosis yields reduced meiotic recombination. Meiotic recombination frequencies between five markers on chromosome II were measured by tetrad disection. Values for genetic distance above 50 cM (gray bar) cannot be distinguished with confidence. Further details are shown in Table S2.

The meiotic bouquet is thought to promote pairing and recombination between homologs, which are in turn crucial for reductional chromosome segregation at meiosis I. We measured intergenic recombination between a number of loci at various positions along chromosome II in the *taz1*Δ*lig4*Δ background (Figure 1C). While the progeny derived from *lig4*Δ meiosis show wild-type (WT) levels of recombination, *taz1*Δ*lig4*Δ meiosis yields a reduction in recombination frequency between two pairs of markers, *leu1-mat1* and *his3-leu1*, both of which lie near the centromere. Recombination within the long interval *leu1-arg4* is frequent enough to guarantee $\geq$1 crossover in this region, although its length prohibits us from assigning significance to differences between strains. We note that we may underestimate deficits in recombination, as we can only assess recombination in colonies produced from viable spores. At a more telomere-proximal region, *taz1*$^+$ deletion does not yield reduced recombination. We speculate that this stems from two competing effects: the loss of Taz1 confers a subtelomeric hyper-recombination phenotype (M.G. Ferreira and J.P.C., unpublished data; Miller et al., 2006), which might counteract any reduction in meiotic recombination conferred by disruption of the bouquet. Thus, while gene conversion frequencies throughout chromosome II are moderately reduced in *taz1*Δ*lig4*Δ strains, at least one crossover is expected to be established and should be sufficient for meiosis I. We also confirmed that reductional segregation occurs properly in those *taz1*Δ *lig4*Δ zygotes that undergo meiosis I (Figure S1).

During the bouquet stage, telomeres associate with the SPB via physical interactions between Taz1, Rap1, Bqt1, and Bqt2 (Chikashige et al., 2006). Rap1 is a Taz1-binding protein whose loss leads to telomere fusions upon G1 arrest as well as a complete loss of bouquet formation. As seen for *taz1*Δ meiosis, the defects in *rap1*Δ meiosis are partially rescued by the concomitant deletion of *lig4*$^+$. *rap1*Δ*lig4*Δ strains show high levels of abnormal asci and reduced levels of meiotic recombination (Figures 1B and 1C). *bqt1*Δ strains, which also completely lack telomere bouquets, show defects in spore formation and meiotic recombination similar to those seen in *rap1*Δ*lig4*Δ strains (Chikashige et al., 2006; Martin-Castellanos et al., 2005; and Figures 1C and S2 and Table S3). Thus, all of the bouquet-defective strains show abnormal ascus formation and reduced meiotic recombination.

To gain perspective on the severity of the recombination deficiency seen in the bouquet-defective strains, we compared them with strains lacking the fission yeast dynein motor protein, Dhc1, which is required for meiotic horsetail movement but not for formation of the bouquet (Figure S2; Yamamoto et al., 1999). *dhc1*Δ meiosis produces largely four-spored asci despite markedly lower levels of meiotic recombination (Yamamoto et al., 1999; Figures 1B and 1C). Thus, bouquet mutants show defects in ascus formation that are disproportionate to their mild defects in recombination.

The foregoing results indicate that *taz1*Δ*lig4*Δ zygotes have a spore formation defect, showing numerous asci in which either meiosis I or meiosis II has failed. Nonetheless, in those *taz1*Δ*lig4*Δ zygotes that do undergo the first meiotic division, chromosomes undergo an accurate reductional segregation. This observation suggests that the defects in *taz1*Δ*lig4*Δ asci cannot be due entirely to defects in homologous recombination. Hence, we performed a detailed live analysis to determine when and how meiotic progression fails.

Bouquet Mutants Have Dysfunctional SPBs

To monitor meiotic progression in live cells, we constructed strains in which one copy of the gene encoding histone H3 is tagged with mRFP (Campbell et al., 2002) and the SPB component Pcp1 (orthologous to budding yeast Spc110; Flory et al., 2002) is tagged at its endogenous locus with GFP (Figure 2). Under the conditions we use for live analysis, most WT cells finish meiosis normally and produce four healthy spores (see Experimental Procedures). Delayed segregation of a fraction of chromosomes (the ''lagging chromosome'' phenotype) is occasionally observed, but this does not affect the final chromosome distribution (Figure S3A). Thus, the experimental stress of repeated exposure to light imposed by timelapse microscopy appears not to significantly affect meiosis.

Pcp1 signals are weak during meiotic prophase in WT cells, and their foci can be seen to migrate back and forth across the zygote as the horsetail nucleus traverses the cell. Throughout this period, chromosome movement follows SPB movement (Figure 2A; ~60 min). The Pcp1 signal intensifies at the end of the horsetail stage (70 min), localizes to the center of the cell, and divides to form two SPB signals that migrate symmetrically to opposite ends of the zygote as it undergoes meiosis I (75~110 min). Then the SPBs duplicate for meiosis II, during which each pair of SPBs remains near the respective tip of the zygote (120~160 min).

In *taz1*Δ*lig4*Δ zygotes, SPBs move normally during the horsetail stage even though they are rarely associated with chromatin. However, as the horsetail stage ends and meiosis I begins, the Pcp1-GFP signals appear brighter than in WT cells and are markedly disorganized (Figure 2B; 75 min). In addition, they frequently fail to localize to opposite ends of the zygote at anaphase I (Figures 2B and 2C). This phenomenon is also observed in *bqt1*Δ single mutant backgrounds (Figure 2D) in which telomere integrity is intact (data not shown), indicating that it stems not from some aspect of the DNA-damage response that occurs at *taz1*Δ telomeres but rather from the failure of these telomeres to form a bouquet. Moreover, similar results were obtained by visualizing the SPB through other tagged SPB components, including Sid4-GFP, Sad1-GFP, and Cut12-GFP (Figure S4; data not shown). Hence, the SPB behaves aberrantly in the absence of stable bouquet formation.

Chromosome segregation defects can also be observed in some *taz1*Δ*lig4*Δ zygotes that contain normal SPB signals. These defects include cases in which chromosomes fail to reach the tips of the zygote and

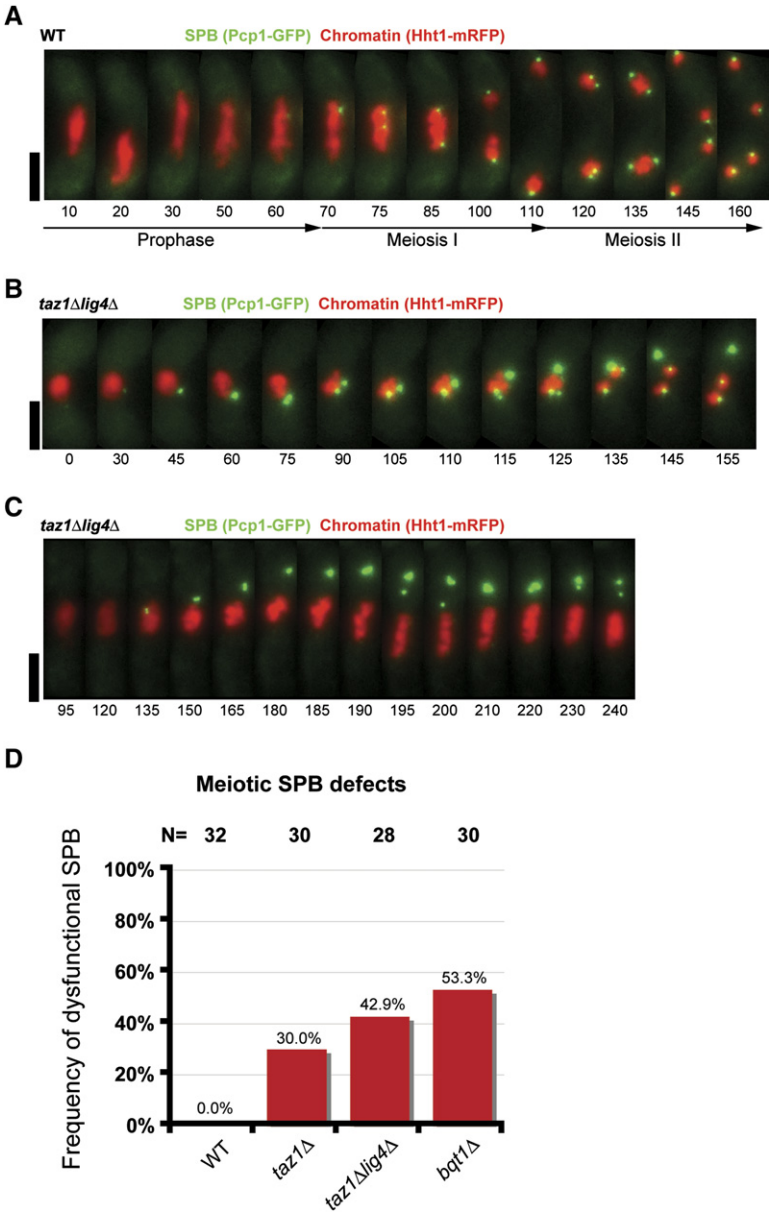

Figure 2. *taz1*Δ*lig4*Δ Zygotes Show Aberrant Meiotic SPB Behavior and Chromosome Missegregation

(A–C) Series of frames from films of meiosis. The SPB and chromosomes were observed via endogenously tagged Pcp1-GFP and Hht1-mRFP, respectively. Numbers below the slides represent minutes elapsed since filming began. Scale bars equal 5 μm.

(A) WT meiosis. The stages of meiosis are indicated below the images.

(B) Aberrant *taz1*Δ*lig4*Δ meiosis in which chromosomes segregate only at meiosis II. At meiosis I, one of the divided SPBs is dysfunctional and dissociates from the nucleus.

(C) In this example, the entire SPB dissociates from chromosomes after chromosome condensation.

(D) Frequency of dysfunctional SPBs observed in Pcp1-GFP Hht1-mRFP zygotes of the indicated genotypes. Other observed phenotypes are summarized in Figure S3D.

repeatedly pull back toward the middle but eventually segregate (Figures S3C and S3E). This rare phenotype is specific to the *taz1*Δ*lig4*Δ background and is not found among *rap1*Δ*lig4*Δ or *bqt1*Δ zygotes (Figure S3D and Table S3). We suspect that this aberrant chromosome behavior stems from the defect in replication fork progression seen in *taz1*Δ cells but not in *rap1*Δ or *bqt1*Δ cells. As expected, chromosome fusions that are not resolved at anaphase are frequently seen in *taz1*Δ meiosis when Lig4 is present (Figure S3B) and the nuclei fail to segregate (Figure S1B).

Bouquet Mutants Fail to Form a Bipolar Spindle

As the SPB nucleates the yeast spindle, we next asked whether the aberrant SPB behavior seen in the absence of a stable bouquet is associated with defective spindle formation. To visualize microtubules, we use strains containing an ectopically integrated copy of the gene encoding α-tubulin fused with GFP (GFP-Atb2; Ding et al., 1998). During WT meiotic prophase I, microtubules move back and forth across the cytoplasm, pulling the horsetail nucleus (Figure 3A; ~55 min). These cytoplasmic microtubules disappear before meiosis I and the nuclear spindle appears as a thick line (65 min). Chromosomes localize to the middle of the spindle at the metaphase plate (85 min) and then segregate to opposite spindle poles (95~105 min). Meiosis II proceeds with a shorter spindle than meiosis I (130~160 min), finally segregating four bunches of chromosomes, each of which is encapsulated within a spore.

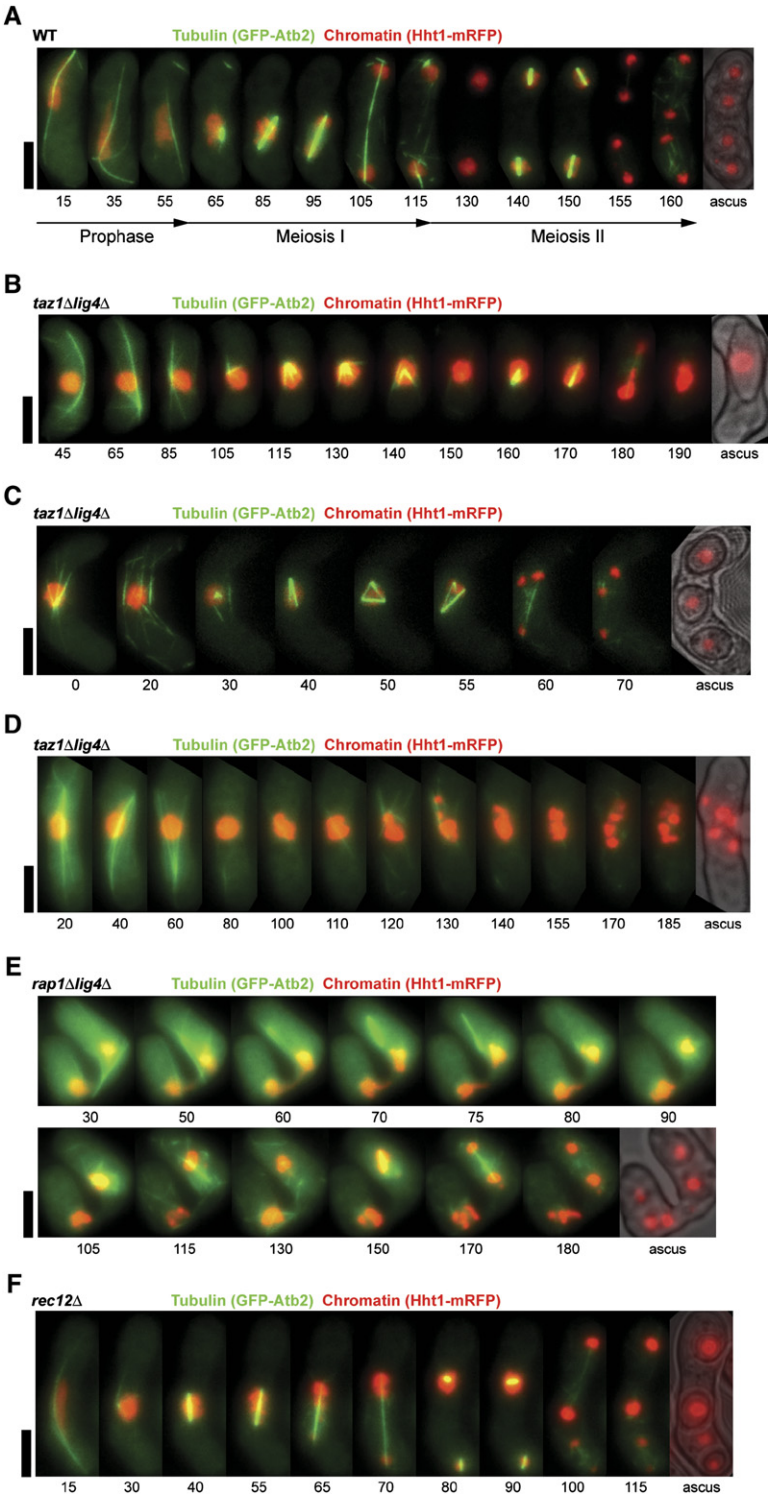

Figure 3. Bouquet Mutants Show Defects in Meiotic Spindle Formation

Frames from films of meiosis. Tubulin and chromosomes are observed via ectopically expressed GFP-Atb2 and endogenously tagged Hht1-mRFP, respectively. Numbers below the slides represent minutes since filming began. Spore formation was photographed approximately 12 hr after filming. Scale bars equal 5 μm.

(A) Bipolar spindles are produced at both meiosis I and meiosis II in WT cells.

(B) Monopolar spindle formation in meiosis I, along with defective chromosome segregation.

(C) Monopolar spindle formation in meiosis I, followed by tri-polar spindle formation at meiosis II, yielding three aberrant spores in this *taz1Δlig4Δ* zygote.

(D) A weak thin spindle has formed from the center of the chromosome mass in this *taz1Δlig4Δ* zygote. Chromosomes are fragmented and no spores are produced.

(E) Example of *rap1Δlig4Δ* meiosis. A spindle forms without attached chromosomes, and a second spindle forms around one mass of chromosomes at meiosis II. The severely bent shape of the zygote shown is not uncommon in bouquet-defective mutants.

(F) *rec12Δ* meiosis. The SPB and spindle behave as they do in WT, but the chromosomes segregate unequally, producing four aberrant spores.

Thirty-seven percent of *taz1Δlig4Δ* zygotes show pronounced defects in spindle formation. Half of these exhibit monopolar spindles (Figure 3B), while smaller fractions show triangular or V-shaped patterns indicating multiple spindles (3.7% of the total, Figure 3C) or a spindle at the wrong position (1.9%, Figure 3E). Others (12.9%) have no visible spindle (Figure 3D). These phenomena were also observed in the other bouquet-deficient strains, *rap1Δlig4Δ* and *bqt1Δ* (Table S3; Figures 3E, 4B, and 4C). A detailed quantitation of the distribution of phenotypes is

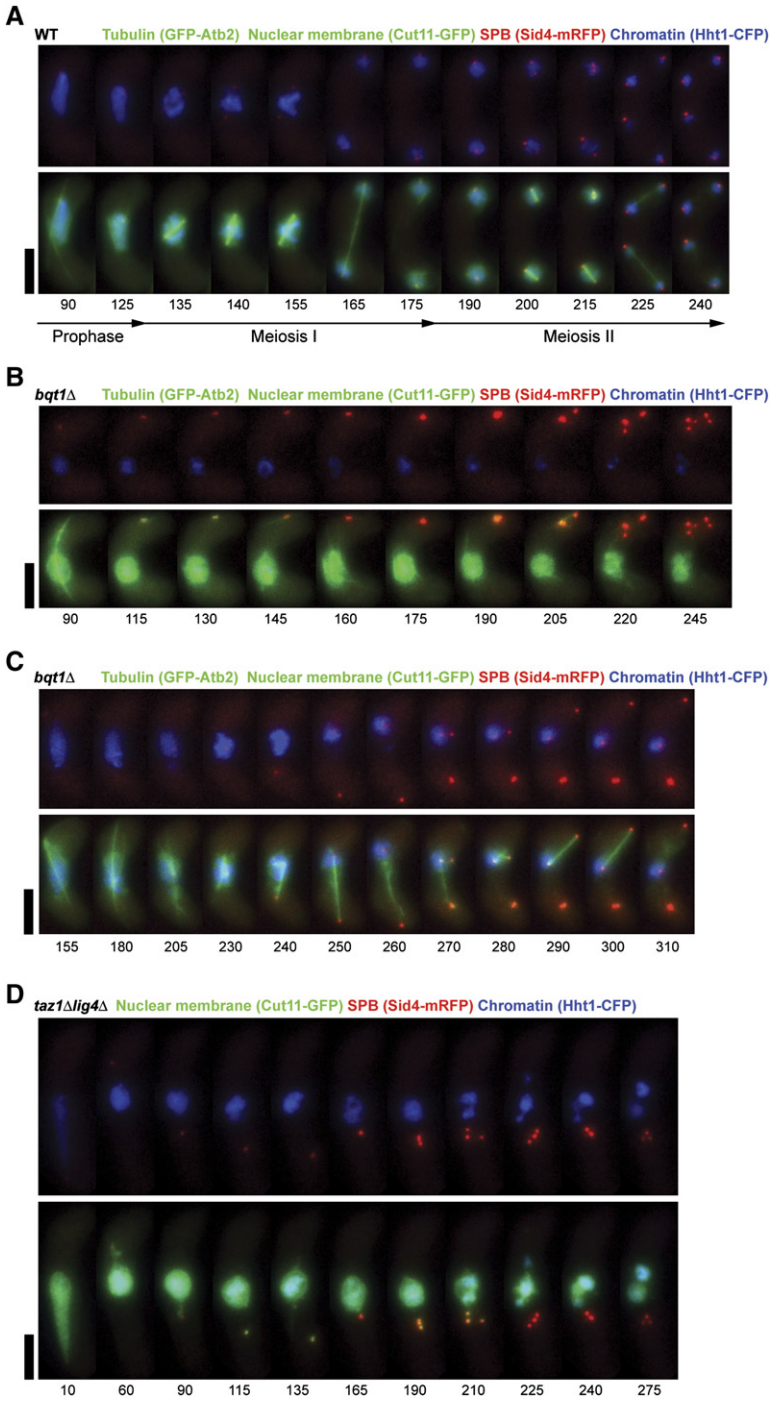

Figure 4. The Meiotic SPB Dissociates from the Nuclear Membrane in Bouquet-Deficient Strains

Frames from films of meiosis. Tubulin, the SPB, and chromosomes were observed via ectopically expressed GFP-Atb2 (A–C) and endogenously tagged Sid4-mRFP and Hht1-CFP, respectively. Cut11, which localizes to the nuclear membrane and, during mitosis or meiosis, to the SPB, was tagged with GFP at its endogenous locus. Scale bars equal 5 μm.

(A) The SPB associates with the nuclear membrane throughout meiosis in WT. Also see Movie S3.

(B) *bqt1*Δ zygote in which the SPB detaches from the nuclear membrane and fragments into five foci. Also see Movie S4.

(C) *bqt1*Δ zygote in which a SPB fragment dissociates from the nucleus. In this case, the spindle elongated as soon as it formed, effectively skipping metaphase. Also see Movie S5.

(D) *taz1*Δ*lig4*Δ zygote in which the Sid4 and Cut11 components of the SPB dissociate from the nucleus. Also see Movie S6.

shown in Table S3. *rap1*Δ*lig4*Δ and *bqt1*Δ strains show higher percentages of all defects than *taz1*Δ*lig4*Δ strains (see also Figures 1B and 2D). This correlates with the relative severity of bouquet disruption seen in these strains—while a residual level of bouquet formation is seen in the absence of Taz1, no bouquet formation is seen in the absence of Rap1 or Bqt1 (Cooper et al., 1998; Nimmo et al., 1998; Chikashige and Hiraoka, 2001; Kanoh and Ishikawa, 2001; Table S3). Likewise, *taz1*Δ*lig4*Δ zygotes sometimes show horsetail movement while *rap1*Δ*lig4*Δ and *bqt1*Δ zygotes do not. Thus, formation of a proper meiotic spindle depends on stable formation of the telomere bouquet.

To further explore the relationship between SPB dysfunction and aberrant spindle formation, we monitored the SPB component Sid4 (Chang and Gould, 2000) and the spindle simultaneously (Figure S4). In WT and *lig4*Δ

meiosis, SPB foci appear at the leading edge of the moving nucleus during the horsetail stage (Ding et al., 1998; Figure S4A and Movie S1). Following SPB division at meiosis I, a bipolar spindle is formed between the two SPBs. In all of 18 observed cells, the SPB remained localized at the tips of the bipolar spindles during WT meiosis I and meiosis II (Figure S4A and Movie S1). Of 68 *taz1*Δ*lig4*Δ zygotes, 58% possessed SPB signals at both tips of a bipolar spindle (Figure S4E). However, in those zygotes that produced a monopolar spindle (13%), at least one SPB focus had become completely detached (Figure S4B and Movie S2). Weak spindle signals lacking any associated Sid4 foci are seen in 25% of cells (Figure S4C). In such cases, the spindles appeared to be nucleated from condensed chromosomes, which align themselves along the spindle but do not segregate properly. Thus, failure to form a telomere bouquet leads to dissociation of SPBs from spindles.

SPBs Detach from the Nuclear Membrane in Bouquet Mutants

The yeast SPB remains embedded in the nuclear membrane throughout WT meiosis. However, our films of SPB and chromatin behavior suggest that the SPB strays from the nucleus in bouquet-deficient zygotes. To address this directly, we visualized the nuclear membrane using Cut11-GFP, which localizes constitutively to the nuclear pore complex (NPC) as well as to the mitotic and meiotic SPBs (West et al., 1998); Sid4-mRFP was used to monitor SPB localization. While the nuclear membrane always surrounds both the SPBs and chromosomes during normal meiosis (Figure 4A, Movie S3), the SPB is often seen outside the nuclear membrane once the horsetail stage has ceased in bouquet mutants. For example, Figure 4B and Movie S4 show a *bqt1*Δ zygote in which the SPB detaches from the nucleus just before meiosis I and becomes fragmented into five foci. In other cases, a bipolar spindle forms at meiosis I, but one of the duplicated SPBs nonetheless dissociates from the nucleus (Figures 4C and S4D and Movie S5). Hence, newly divided SPBs are not stably connected to the nuclear membrane in cells lacking a bouquet. To confirm these observations, we visualized the nuclear membrane using a GFP-tagged peptide that localizes to all membranes in the cell. Staining with this marker again reveals separation of the SPB from the nucleus following SPB division in *rap1*Δ*lig4*Δ zygotes (Figures S5A and S5B). Hence, in the absence of a stable bouquet, dysfunctional SPBs become disconnected from the nuclear membrane after meiotic prophase.

To determine whether the entire SPB complex is disconnected from the membrane in the absence of the bouquet, we asked whether Cut11-GFP foci appear at the dissociated SPB using strains without GFP-Atb2 expression (Figure 4D), as the fluorescent microtubules obscure localization of SPB-associated Cut11-GFP. In addition to localizing to the nuclear membrane, Cut11 appears at the SPB just as it divides before meiosis I (yellow foci indicating colocalization of Cut11 and Sid4, Figure 4D; 115∼135 min and Movie S6) and again at the meiosis II division (190∼210 min). Like the Sid4 component of the SPB, Cut11 is dislodged from the nucleus in a *taz1*Δ*lig4*Δ background. Furthermore, we confirmed that the SPB components Pcp1 and Sad1 become disconnected from the nuclear membrane (Figure S5C; data not shown). These results suggest that the entire SPB is destabilized and detached from the nuclear membrane in the absence of the bouquet.

Dysfunctional SPB and Spindle Behavior Are Independent of Defects in Meiotic Recombination

All of the bouquet-deficient mutants have lower levels of recombination than WT cells. To determine whether the SPB and spindle defects exhibited by bouquet-defective strains are indirect effects of problematic recombination, we monitored SPBs and microtubules in strains lacking Rec12 or Dhc1. Both *rec12*Δ and *dhc1*Δ zygotes show proper bouquet formation along with normal SPB behavior and bipolar spindle formation (Figures 3F and S2; Table S3). Indeed, in these mutants, chromosome segregation patterns are clearly defective despite the presence of relatively normal spindles. Thus, the dysfunctional SPB and spindle formation defects seen in zygotes lacking stable telomere bouquets were not secondary effects of reduced meiotic recombination. Rather, these defects are likely to stem from the lack of a physical connection between telomeres and SPBs.

During WT meiotic prophase, the SPB is pulled across the zygote by the dynein motor (Yamamoto et al., 1999). In bouquet-defective strains, the mass of chromatin remains in the middle of the zygote even though the SPB continually traverses it, carrying a section of nuclear membrane and thereby stretching the nucleus (Figure 4E; ∼90 min). Conceivably, this situation might lead to tearing of the nuclear membrane or SPB detachment, resulting in the wandering SPB and spindle formation failure that we observe. If this were true, these defects should be suppressed by preventing horsetail movement via deletion of *dhc1*$^{+}$. To test this possibility, we monitored chromatin and spindle movements in cells lacking not only the bouquet-forming apparatus but also Dhc1 (i.e., *taz1*Δ*lig4*Δ*dhc1*Δ and *bqt1*Δ*dhc1*Δ). Live analysis revealed the same SPB and spindle defects in bouquet mutants containing or lacking Dhc1 (Figure S6), indicating that the dissociation of the SPB from the nucleus is not caused by the force of horsetail movement.

Telomeres Dissociate from the SPB at Meiosis I: Telomere Fireworks

While the bouquet exists throughout meiotic prophase, our foregoing observations suggest that defective bouquet formation has repercussions for events that follow meiotic prophase. To investigate the timing of bouquet dissolution, SPB division, and spindle formation more closely, we filmed telomeres (via Taz1-GFP) along with the SPB in a WT background (Figure 5A). During meiotic

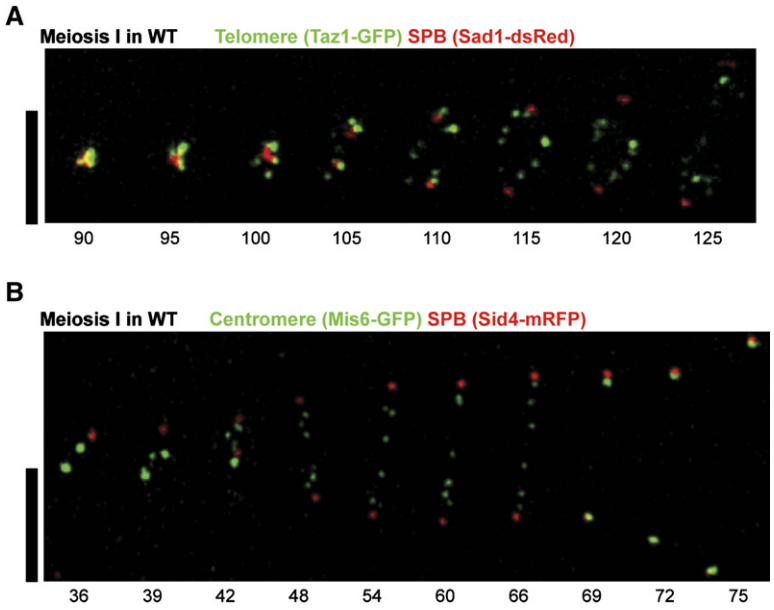

Figure 5. Telomere Fireworks

All the telomeres in the bouquet dissociate from the SPB simultaneously with SPB division in WT zygotes. Frames of films running from pre-meiosis I to anaphase I are shown. Three-dimensional data are deconvolved and reconstructed as a flattened image. Telomeres, centromeres, and SPBs are observed via endogenously tagged Taz1-GFP, Mis6-GFP, and Sad1-dsRed or Sid4-mRFP, respectively. Numbers below the frames represent minutes since filming began. Scale bars equal 5 μm.

(A) Telomeres dissociate simultaneously with SPB division.

(B) Centromeres do not reassociate with the SPB before its division.

prophase, the telomeres are tightly associated with the SPB. However, just before meiosis I, all of the telomeres dissociate in a concerted manner from the SPB. As the telomeres dissociate, they disperse into a symmetrical pattern around the SPB that resembles fireworks; hence, we refer to the dissolution of the telomere bouquet as "telomere fireworks" (Figure 5A). Telomere fireworks immediately precede SPB division. This result was confirmed by GFP-tagging an alternative telomere-binding protein, Pot1 (Baumann and Cech, 2001), indicating that the telomere fireworks represent movements of the entire telomere complex. The close correspondence between the timing of telomere fireworks and SPB division suggests that the two events are functionally coupled.

Centromeres Do Not Reassociate with the SPB prior to Meiosis I

Conceivably, the aberrant meiosis seen in bouquet-deficient strains might stem from a requirement for telomeres to exchange SPB association with centromeres prior to meiosis I. To ask whether centromere reassociation with the SPB is essential for proper SPB behavior, we examined this period in a strain carrying a GFP tag on the kinetochore protein Mis6 (Saitoh et al., 1997) as well as Sid4-mRFP. In 12 of 14 cells examined, the centromeres colocalized with Sid4-mRFP only after SPB division (Figure 5B). We also monitored centromere 1 reassociation with the SPB by timelapse microscopy in 1 min intervals and confirmed that centromere reassociation occurs after SPB division (data not shown). Hence, rather than the centromeres reassociating with the SPB before meiosis I, it appears that the centromeres associate with the spindle subsequent to its formation and are later pulled to the divided SPBs. This result suggests that spindle formation in meiosis I neither correlates with nor requires centromere-SPB reassociation.

Meiotic Spindle Formation Is Not Supported by Telomere Proteins without Attached Telomeres

We wondered if proper spindle behavior during meiosis requires the actual association of telomeres and the SPB to form a bouquet, or whether it simply requires recruitment of a Bqt1-Rap1-Taz1 protein complex to the meiotic SPB. To address this question, we used an allele of *taz1*, *taz1-A606V*, which harbors a point mutation within the Myb DNA-binding domain that disrupts DNA-binding activity in vitro (A. Deshpande and J.P.C., unpublished data) and confers many features of the *taz1*Δ phenotype in vivo, including the telomere-SPB clustering defect (Nimmo et al., 1998). We first checked localization of Taz1-A606V using a strain in which the *taz1*$^{+}$ gene is replaced with DNA encoding Taz1-A606V-GFP. During mitotic interphase, Taz1-A606V-GFP is seen diffusely throughout the nucleoplasm, occasionally forming a faint focus at the periphery (Figure S7). In contrast, during meiotic prophase, Taz1-A606V localizes to the SPB, with some cells showing additional foci (Figures 6A, 6B, and S7). Chromatin clearly fails to colocalize with SPB-associated Taz1-A606V, confirming that this allele lacks the ability to bind telomeres. This behavior resembles that of Rap1 in meiotic *taz1*Δ cells (Chikashige and Hiraoka, 2001; Kanoh and Ishikawa, 2001), suggesting that Rap1 recruits Taz1-A606V to the SPB. Indeed, we never observe Taz1-A606V-GFP foci in a *rap1*Δ background (Figures 6B and S7). Hence, while Taz1-A606V-GFP is unable to bind telomeres, it appears to retain the ability to associate with the meiotic prophase SPB in a Rap1-dependent manner, providing an experimental tool for addressing whether Taz1 confers proper SPB and spindle behavior in the absence of bound telomeres.

As *taz1-A606V* confers the accumulation of telomere-telomere fusions in G1-arrested cells (our unpublished data), we monitored meiosis in a *taz1-A606V-GFPlig4*Δ

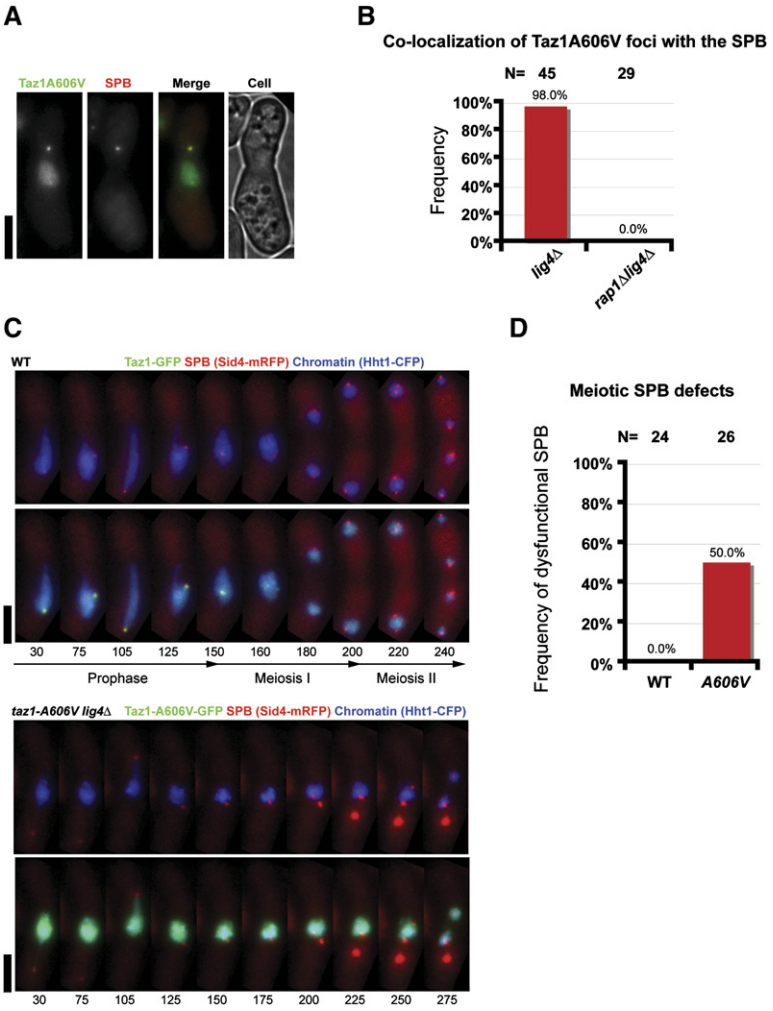

Figure 6. Meiotic Spindle Formation Is Not Promoted by Telomere Proteins without Attached Telomeres

(A and B) Taz1-A606V-GFP binds the meiotic SPB (Sid4-mRFP) in a Rap1-dependent manner.

(A) Example of Taz1-A606V-GFP localization during meiotic prophase (see also Figure S7). Scale bar = 5 μm.

(B) Graph showing the percentage of horsetail stage zygotes in which a Taz1-A606V-GFP focus associates with the SPB.

(C and D) Taz1-GFP and Taz1-A606V-GFP behavior through meiosis. SPBs and chromosomes are observed via endogenously tagged Sid4-mRFP and Hht1-CFP, respectively. GFP fluorescence cannot be captured in isolation as the GFP filter captures CFP fluorescence as well. Cells containing Taz1-GFP without Hht1-CFP are shown in (A) and Figure S7. While Taz1-A606V-GFP localizes to the SPB during meiotic prophase, it fails to bind telomeric DNA and confers SPB defects similar to those of *taz1Δlig4Δ* strains. Scale bars equal 5 μm.

(D) Frequency of dysfunctional SPBs observed via Sid4-mRFP and Hht1-CFP using strains shown in (C).

background. Like *taz1Δlig4Δ* zygotes, 50% of *taz1-A606V-GFPlig4Δ* zygotes show dysfunctional SPBs and form aberrant asci (Figures 6C and 6D). Furthermore, *taz1-A606V-GFPlig4Δ* zygotes suffer spindle aberrations similar to those of *taz1Δlig4Δ* cells (Table S3). Thus, the presence of the Taz1-A606V, Rap1, and Bqt1 proteins at the SPB is not sufficient to confer proper meiotic SPB and spindle behavior. A caveat to this observation is that we do not know whether the levels of Taz1-A606V at the meiotic SPB are comparable to the levels of Taz1 at the SPB in WT cells. However, this result suggests that successful spindle formation requires not only SPB-associated Taz1 but also that the Taz1 complex is bound to telomeres and confers the bouquet chromosome geometry.

DISCUSSION

Bouquet Formation Is Required for Proper Meiotic SPB and Spindle Behavior

The meiotic bouquet has been traditionally assumed to function in promoting recombination. However, bouquet-defective mutants show only mild defects in meiotic recombination while producing highly defective asci, leading us to suspect additional roles for the bouquet. Using timelapse live analysis, we observe striking defects in SPB and spindle behavior in bouquet-deficient mutants, and these are not secondary to defects in meiotic recombination. Hence, our results challenge the notion that facilitation of homolog pairing is the primary function of the bouquet and suggest instead that the clustered telomeres are crucial for promoting the formation of a bipolar meiotic spindle.

SPB behavior during the horsetail stage appears normal in the absence of a stable bouquet, as the SPB oscillates normally during this period in bouquet-defective mutants, remaining within a section of nuclear membrane even though it is unconnected to chromosomes. However, just prior to the onset of meiosis I, we see a severe departure from normal SPB behavior in bouquet-defective strains. Unusually bright SPB foci appear and frequently show fragmentation and mislocalization. Importantly, this period corresponds to the moment of telomere fireworks, the concerted dissociation of telomeres from the

SPB that immediately precedes SPB division in WT cells (Figure 5A). Hence, it is tempting to speculate that the presence, or the dissociation, of the bouquet triggers a signal within the SPB that elicits its division. Furthermore, the SPBs often detach from the nuclear membrane and localize to the cytoplasm in the absence of the bouquet. Thus, in the absence of a stable bouquet, the SPB appears deregulated in several senses: it accrues an excessive amount of SPB components, breaks into irregular fragments, and strays from the nucleus. These results implicate bouquet formation in the maturation and nuclear integration of the meiotic SPB. Intriguingly, in the absence of the bouquet, nuclear anchoring of the SPB at meiosis I does not guarantee anchoring at meiosis II. This suggests that the bouquet makes some mark on the SPB that persists through meiosis II and argues against a model in which the bouquet-dependent event is the meiosis I attachment of the SPB to the nuclear membrane.

Dysfunctional SPBs and spindles have been observed previously in a number of settings. The monopolar spindle that often emanates from a bouquet-defective zygote's single functional SPB (Figure S4B) resembles the monopolar mitotic spindles seen in cells harboring mutations in the SPB components Sad1, Cut11, or Cut12 (Bridge et al., 1998; Hagan and Yanagida, 1995; West et al., 1998). Moreover, in *cut11* mutants, SPB detachment from the nuclear membrane is observed (West et al., 1998). Thus, upsetting the balance of SPB components may elicit defects in the anchoring of SPBs to the nuclear membrane. Conceivably, the bouquet impinges on this balance, as suggested by the excess accumulation of SPB components seen in bouquet-defective strains. These observations are reminiscent of the appearance of aberrant meiotic MTOCs seen upon loss of Dot2, a transcription factor that represses expression of *pcp1*$^{+}$ (Jin et al., 2005). Perhaps the bouquet acts in concert with Dot2 to halt the stockpiling of SPB components and thereby regulate SPB maturation.

The molecular feature of the bouquet that is crucial for SPB maturation remains a mystery. Our data suggest that association of bona fide telomeres with the SPB is crucial, as proper SPB and spindle behavior fail to be conferred by recruitment of a nontelomeric DNA-bound Taz1-Rap1-Bqt complex. Nonetheless, it is conceivable that stable association of any heterochromatic region with the SPB would support meiotic spindle function, or that association of any chromosomal region would suffice. Alternatively, chromosome end-clustering may be required to impart a mechanical pulling force on the SPB that triggers its maturation, or some component of the SPB may become modified by a telomeric factor that can only act in the context of a bona fide telomere complex.

Why Switch Cenromere and Telomere Positions during Meiotic Prophase?

During the mitotic cell cycle, interphase centromeres localize near the SPB and telomeres remain at distinct sites along the nuclear periphery. Our data suggest the possibility that this centromere-SPB association controls maturation and division of the mitotic SPB. If mitotic centromeres and meiotic telomeres were to play similar roles in promoting spindle formation, it would be pertinent to ask why a switch between centromeres and telomeres has evolved. We speculate that the answer lies in the organization of a reductional nuclear division. In order to confer this highly specialized segregation pattern, the meiotic centromere is fully covered with the meiosis-specific cohesin, Rec8 (Watanabe and Nurse, 1999). This in turn recruits Shugoshin, the protein that protects centromeric sister cohesion until meiosis II (Kitajima et al., 2004), and Moa1, which ensures that sister kinetochores attach to the same spindle pole at meiosis I (Yokobayashi and Watanabe, 2005). In addition to enforcing monopolar spindle attachment, sister cohesion, and homolog dysjunction during meiosis I, centromeres play crucial roles in the pairing of homologs as well as nonexchange chromosomes (Ding et al., 2004). Hence, bouquet formation may have evolved to allow centromeres to engage in this extensive array of meiotic activities. Importantly, *taz1*Δ*lig4*Δ zygotes that undergo meiosis I do so with a proper reductional chromosome segregation (Figure S1). However, we suggest that if the centromere remained associated with the SPB during meiotic prophase, the ability of centromeres to organize meiosis I would be compromised. For example, binding of centromeres to the SPB may involve protein interactions that would sterically block the association of one or more meiosis-specific kinetochore-associated factors.

Prospects for Understanding the Conserved Functions of the Bouquet

In budding yeast, Ndj1 has been suggested to function similarly to the fission yeast Bqt complex. Ndj1 is expressed specifically during meiotic prophase, localizes at telomeres, and has a deletion phenotype that partially parallels those of the bouquet-defective strains described herein. The fission yeast Bqt complex directly contacts Sad1, which is a member of the SUN-domain family of proteins generally involved in linking the nuclear membrane to cytoskeletal or chromosomal elements. Likewise, Ndj1 interacts with a SUN-domain protein (Mps3) in a two-hybrid assay (Ito et al., 2001). Furthermore, *ndj1* deletion leads to a defect in bouquet formation (Chua and Roeder, 1997; Conrad et al., 1997; Trelles-Sticken et al., 2000). However, some *ndj1* phenotypes differ from those of *taz1*Δ*lig4*Δ, *rap1*Δ*lig4*Δ, and *bqt1*Δ cells. Cells lacking Ndj1p show homolog nondysjunction as well as delays in both meiotic prophase progression (Chua and Roeder, 1997; Conrad et al., 1997) and DSB repair (Wu and Burgess, 2006). In contrast, *taz1*Δ zygotes show no delay in meiotic prophase (Ding et al., 2004), and *bqt1*Δ zygotes show normal frequency and timing of DSB repair (Martin-Castellanos et al., 2005). Thus, Ndj1 may promote meiosis through multiple roles, some dependent on and some independent of bouquet formation.

The universal features of meiotic spindle formation have yet to be determined; nonetheless, modulation of this process by the bouquet may occur in many eukaryotes. In higher eukaryotes, meiotic spindles can be nucleated from several different structures, including centrosomes, MTOCs, and complexes of motor proteins. During mouse oogenesis, meiotic spindle formation occurs in the absence of centrioles but in the presence of multiple MTOCs (Maro et al., 1985; Messinger and Albertini, 1991); our data would suggest that those MTOCs that form the spindle are marked by the telomere bouquet. In *Xenopus* egg extracts, spindles are nucleated by chromosomes (Heald et al., 1996), and spindle formation continues after laser ablation of MTOCs in mammalian and dipteran cell lines (Khodjakov et al., 2000; Mahoney et al., 2006). However, these spindles are not properly organized and the efficiency of spindle formation is enhanced by MTOCs. These phenomena may be analogous to those observed in bouquet-defective fission yeast, in which nonfunctional meiotic spindles appear to emanate both from chromosomes and from SPBs that are aberrantly located in the cytoplasm. Hence, this study raises the possibility that control of spindle nucleation by the highly conserved telomere bouquet is a widespread phenomenon. In the absence of communication between the bouquet and the spindle-nucleation apparatus, spindles may form, but they are unable to efficiently organize chromosomes.

Information on the determinants of bouquet formation in metazoan organisms has started to trickle in. In both mice and maize, mutations that compromise synapsis show delayed progression out of the bouquet stage (Golubovskaya et al., 2002; Liebe et al., 2004), but mutants that specifically affect the bouquet are not yet available. TRF1 and TRF2, the mammalian orthologs of Taz1, have been shown to localize to telomeres throughout both mitotic and meiotic cell cycles (Bilaud et al., 1997; Broccoli et al., 1997; Chong et al., 1995; Scherthan et al., 2000), and given the many parallels between Taz1 and TRF function, we can anticipate that the TRFs will be involved in bouquet formation. However, the meiotic effects of inhibiting the TRFs are not yet known. Here, we show that telomere clustering influences the architecture of the meiotic SPB and spindle, along with their localization within or outside of the nucleus. Hence, this work reveals a previously unrecognized function for the bouquet that is likely to be relevant to mammalian meiosis as well and raises new questions about communication between chromosomes and microtubules through the cell cycle.

EXPERIMENTAL PROCEDURES

Microscopy and Live Cell Imaging

Details of strain construction are presented in Supplemental Experimental Procedures. Live analysis was carried out by adhering cells to 35 mm glass culture dishes (MatTek) precoated with 0.2 mg/ml soybean lectin (Calbiochem) and immersing them in EMM-N with required supplements (+0.2 μM thiamine for Pnmt1-GFP-Atb2).

Imaging was carried out with a DeltaVision Spectris (Applied Precision) comprising an Olympus IX71 wide-field inverted fluorescence microscope, an Olympus UPlanSApo 100×, NA 1.35, oil immersion objective, and a Photometrics CCD CH350 camera cooled to −35°C (Roper Scientific). Culture dishes were incubated at 28°C in the Environmental Chamber. Images were captured and analyzed using SoftWoRx (Applied Precision). Series of telomere fireworks images were captured with 0.3 s exposure per plane at a 0.3 μm step size over 25 focal planes; this was repeated every 5 min for 3 hr. Series of centromere reassociation images were captured with 0.3 seconds exposure per plane at a 0.3μm step size over 21 focal planes; this was repeated every 3 minutes for 2 hours. Series documenting SPB detachment using pD817 as a membrane marker were captured with 0.3 s exposure per plane at a 0.3 μm step size over 21 focal planes; this was repeated every 10 min for 5 hr. These images were deconvolved and combined into maximal intensity projections. For long-term time-course experiments, 7.2 μm of z axis imaging was acquired with Optical Axis Integration (OAI), which acquires a projected image of the z axis using a continuous Z sweep. Coverage of the entire cell required a sweep lasting approximately 3 s, and this was repeated every 5 min for approximately 5 hr. Sporulated asci were photographed as bright-field or DIC images approximately 12 hr later.

Supplemental Data

Supplemental Data include Supplemental Experimental Procedures, seven figures, two tables, and six movies and can be found with this article online at http://www.cell.com/cgi/content/full/130/1/113/DC1/.

ACKNOWLEDGMENTS

We thank Rafael Carazo-Salas and our lab members for discussion and suggestions on the manuscript; Zac Cande, Iain Hagan, Yasushi Hiraoka, and Takashi Toda for the generous gift of strains; Roger Tsien for kindly providing mRFP; and Rebecca Heald, Martin Kupiec, and Takashi Toda for critical comments on the manuscript. This work was funded by Cancer Research UK and the Naito Foundation.

Received: November 17, 2006
Revised: March 7, 2007
Accepted: May 3, 2007
Published: July 12, 2007

REFERENCES

Baumann, P., and Cech, T.R. (2001). Pot1, the putative telomere end-binding protein in fission yeast and humans. Science *292*, 1171–1175.

Bilaud, T., Brun, C., Ancelin, K., Koering, C.E., Laroche, T., and Gilson, E. (1997). Telomeric localization of TRF2, a novel human telobox protein. Nat. Genet. *17*, 236–239.

Bridge, A.J., Morphew, M., Bartlett, R., and Hagan, I.M. (1998). The fission yeast SPB component Cut12 links bipolar spindle formation to mitotic control. Genes Dev. *12*, 927–942.

Broccoli, D., Smogorzewska, A., Chong, L., and de Lange, T. (1997). Human telomeres contain two distinct Myb-related proteins, TRF1 and TRF2. Nat. Genet. *17*, 231–235.

Campbell, R.E., Tour, O., Palmer, A.E., Steinbach, P.A., Baird, G.S., Zacharias, D.A., and Tsien, R.Y. (2002). A monomeric red fluorescent protein. Proc. Natl. Acad. Sci. USA *99*, 7877–7882.

Chang, L., and Gould, K.L. (2000). Sid4p is required to localize components of the septation initiation pathway to the spindle pole body in fission yeast. Proc. Natl. Acad. Sci. USA *97*, 5249–5254.

Chikashige, Y., and Hiraoka, Y. (2001). Telomere binding of the Rap1 protein is required for meiosis in fission yeast. Curr. Biol. *11*, 1618–1623.

Chikashige, Y., Ding, D.Q., Funabiki, H., Haraguchi, T., Mashiko, S., Yanagida, M., and Hiraoka, Y. (1994). Telomere-led premeiotic chromosome movement in fission yeast. Science *264*, 270–273.

Chikashige, Y., Ding, D.Q., Imai, Y., Yamamoto, M., Haraguchi, T., and Hiraoka, Y. (1997). Meiotic nuclear reorganization: switching the position of centromeres and telomeres in the fission yeast Schizosaccharomyces pombe. EMBO J. *16*, 193–202.

Chikashige, Y., Tsutsumi, C., Yamane, M., Okamasa, K., Haraguchi, T., and Hiraoka, Y. (2006). Meiotic proteins bqt1 and bqt2 tether telomeres to form the bouquet arrangement of chromosomes. Cell *125*, 59–69.

Chong, L., van Steensel, B., Broccoli, D., Erdjument-Bromage, H., Hanish, J., Tempst, P., and de Lange, T. (1995). A human telomeric protein. Science *270*, 1663–1667.

Chua, P.R., and Roeder, G.S. (1997). Tam1, a telomere-associated meiotic protein, functions in chromosome synapsis and crossover interference. Genes Dev. *11*, 1786–1800.

Conrad, M.N., Dominguez, A.M., and Dresser, M.E. (1997). Ndj1p, a meiotic telomere protein required for normal chromosome synapsis and segregation in yeast. Science *276*, 1252–1255.

Cooper, J.P., Nimmo, E.R., Allshire, R.C., and Cech, T.R. (1997). Regulation of telomere length and function by a Myb-domain protein in fission yeast. Nature *385*, 744–747.

Cooper, J.P., Watanabe, Y., and Nurse, P. (1998). Fission yeast Taz1 protein is required for meiotic telomere clustering and recombination. Nature *392*, 828–831.

De Veaux, L.C., Hoagland, N.A., and Smith, G.R. (1992). Seventeen complementation groups of mutations decreasing meiotic recombination in Schizosaccharomyces pombe. Genetics *130*, 251–262.

Ding, D.Q., Chikashige, Y., Haraguchi, T., and Hiraoka, Y. (1998). Oscillatory nuclear movement in fission yeast meiotic prophase is driven by astral microtubules, as revealed by continuous observation of chromosomes and microtubules in living cells. J. Cell Sci. *111*, 701–712.

Ding, D.Q., Yamamoto, A., Haraguchi, T., and Hiraoka, Y. (2004). Dynamics of homologous chromosome pairing during meiotic prophase in fission yeast. Dev. Cell *6*, 329–341.

Ding, R., West, R.R., Morphew, D.M., Oakley, B.R., and McIntosh, J.R. (1997). The spindle pole body of Schizosaccharomyces pombe enters and leaves the nuclear envelope as the cell cycle proceeds. Mol. Biol. Cell *8*, 1461–1479.

Ferreira, M.G., and Cooper, J.P. (2001). The fission yeast Taz1 protein protects chromosomes from Ku-dependent end-to-end fusions. Mol. Cell *7*, 55–63.

Flory, M.R., Morphew, M., Joseph, J.D., Means, A.R., and Davis, T.N. (2002). Pcp1p, an Spc110p-related calmodulin target at the centrosome of the fission yeast Schizosaccharomyces pombe. Cell Growth Differ. *13*, 47–58.

Funabiki, H., Hagan, I., Uzawa, S., and Yanagida, M. (1993). Cell cycle-dependent specific positioning and clustering of centromeres and telomeres in fission yeast. J. Cell Biol. *121*, 961–976.

Golubovskaya, I.N., Harper, L.C., Pawlowski, W.P., Schichnes, D., and Cande, W.Z. (2002). The pam1 gene is required for meiotic bouquet formation and efficient homologous synapsis in maize (Zea mays L.). Genetics *162*, 1979–1993.

Hagan, I., and Yanagida, M. (1995). The product of the spindle formation gene sad1+ associates with the fission yeast spindle pole body and is essential for viability. J. Cell Biol. *129*, 1033–1047.

Harper, L., Golubovskaya, I., and Cande, W.Z. (2004). A bouquet of chromosomes. J. Cell Sci. *117*, 4025–4032.

Heald, R., Tournebize, R., Blank, T., Sandaltzopoulos, R., Becker, P., Hyman, A., and Karsenti, E. (1996). Self-organization of microtubules into bipolar spindles around artificial chromosomes in Xenopus egg extracts. Nature *382*, 420–425.

Ito, T., Chiba, T., Ozawa, R., Yoshida, M., Hattori, M., and Sakaki, Y. (2001). A comprehensive two-hybrid analysis to explore the yeast protein interactome. Proc. Natl. Acad. Sci. USA *98*, 4569–4574.

Jin, Y., Mancuso, J.J., Uzawa, S., Cronembold, D., and Cande, W.Z. (2005). The fission yeast homolog of the human transcription factor EAP30 blocks meiotic spindle pole body amplification. Dev. Cell *9*, 63–73.

Kanoh, J., and Ishikawa, F. (2001). spRap1 and spRif1, recruited to telomeres by Taz1, are essential for telomere function in fission yeast. Curr. Biol. *11*, 1624–1630.

Khodjakov, A., Cole, R.W., Oakley, B.R., and Rieder, C.L. (2000). Centrosome-independent mitotic spindle formation in vertebrates. Curr. Biol. *10*, 59–67.

Kitajima, T.S., Kawashima, S.A., and Watanabe, Y. (2004). The conserved kinetochore protein shugoshin protects centromeric cohesion during meiosis. Nature *427*, 510–517.

Liebe, B., Alsheimer, M., Hoog, C., Benavente, R., and Scherthan, H. (2004). Telomere attachment, meiotic chromosome condensation, pairing, and bouquet stage duration are modified in spermatocytes lacking axial elements. Mol. Biol. Cell *15*, 827–837.

Mahoney, N.M., Goshima, G., Douglass, A.D., and Vale, R.D. (2006). Making microtubules and mitotic spindles in cells without functional centrosomes. Curr. Biol. *16*, 564–569.

Maro, B., Howlett, S.K., and Webb, M. (1985). Non-spindle microtubule organizing centers in metaphase II-arrested mouse oocytes. J. Cell Biol. *101*, 1665–1672.

Martin-Castellanos, C., Blanco, M., Rozalen, A.E., Perez-Hidalgo, L., Garcia, A.I., Conde, F., Mata, J., Ellermeier, C., Davis, L., San-Segundo, P., et al. (2005). A large-scale screen in *S. pombe* identifies seven novel genes required for critical meiotic events. Curr. Biol. *15*, 2056–2062.

Messinger, S.M., and Albertini, D.F. (1991). Centrosome and microtubule dynamics during meiotic progression in the mouse oocyte. J. Cell Sci. *100*, 289–298.

Miki, F., Okazaki, K., Shimanuki, M., Yamamoto, A., Hiraoka, Y., and Niwa, O. (2002). The 14-kDa dynein light chain-family protein Dlc1 is required for regular oscillatory nuclear movement and efficient recombination during meiotic prophase in fission yeast. Mol. Biol. Cell *13*, 930–946.

Miller, K.M., Rog, O., and Cooper, J.P. (2006). Semi-conservative DNA replication through telomeres requires Taz1. Nature *440*, 824–828.

Niccoli, T., Yamashita, A., Nurse, P., and Yamamoto, M. (2004). The p150-Glued Ssm4p regulates microtubular dynamics and nuclear movement in fission yeast. J. Cell Sci. *117*, 5543–5556.

Nimmo, E.R., Pidoux, A.L., Perry, P.E., and Allshire, R.C. (1998). Defective meiosis in telomere-silencing mutants of Schizosaccharomyces pombe. Nature *392*, 825–828.

Saito, T.T., Tougan, T., Okuzaki, D., Kasama, T., and Nojima, H. (2005). Mcp6, a meiosis-specific coiled-coil protein of Schizosaccharomyces pombe, localizes to the spindle pole body and is required for horsetail movement and recombination. J. Cell Sci. *118*, 447–459.

Saito, T.T., Okuzaki, D., and Nojima, H. (2006). Mcp5, a meiotic cell cortex protein, is required for nuclear movement mediated by dynein and microtubules in fission yeast. J. Cell Biol. *173*, 27–33.

Saitoh, S., Takahashi, K., and Yanagida, M. (1997). Mis6, a fission yeast inner centromere protein, acts during G1/S and forms specialized chromatin required for equal segregation. Cell *90*, 131–143.

Scherthan, H., Jerratsch, M., Li, B., Smith, S., Hulten, M., Lock, T., and de Lange, T. (2000). Mammalian meiotic telomeres: protein composition and redistribution in relation to nuclear pores. Mol. Biol. Cell *11*, 4189–4203.

Shimanuki, M., Miki, F., Ding, D.Q., Chikashige, Y., Hiraoka, Y., Horio, T., and Niwa, O. (1997). A novel fission yeast gene, kms1+, is required for the formation of meiotic prophase-specific nuclear architecture. Mol. Gen. Genet. *254*, 238–249.

Tanaka, K., Kohda, T., Yamashita, A., Nonaka, N., and Yamamoto, M. (2005). Hrs1p/Mcp6p on the meiotic SPB organizes astral microtubule arrays for oscillatory nuclear movement. Curr. Biol. *15*, 1479–1486.

Tang, X., Jin, Y., and Cande, W.Z. (2006). Bqt2p is essential for initiating telomere clustering upon pheromone sensing in fission yeast. J. Cell Biol. *173*, 845–851.

Trelles-Sticken, E., Dresser, M.E., and Scherthan, H. (2000). Meiotic telomere protein Ndj1p is required for meiosis-specific telomere distribution, bouquet formation and efficient homologue pairing. J. Cell Biol. *151*, 95–106.

Tuzon, C.T., Borgstrom, B., Weilguny, D., Egel, R., Cooper, J.P., and Nielsen, O. (2004). The fission yeast heterochromatin protein Rik1 is required for telomere clustering during meiosis. J. Cell Biol. *165*, 759–765.

Watanabe, Y., and Nurse, P. (1999). Cohesin Rec8 is required for reductional chromosome segregation at meiosis. Nature *400*, 461–464.

West, R.R., Vaisberg, E.V., Ding, R., Nurse, P., and McIntosh, J.R. (1998). cut11(+): A gene required for cell cycle-dependent spindle pole body anchoring in the nuclear envelope and bipolar spindle formation in Schizosaccharomyces pombe. Mol. Biol. Cell *9*, 2839–2855.

Wu, H.Y., and Burgess, S.M. (2006). Ndj1, a telomere-associated protein, promotes meiotic recombination in budding yeast. Mol. Cell. Biol. *26*, 3683–3694.

Yamamoto, A., West, R.R., McIntosh, J.R., and Hiraoka, Y. (1999). A cytoplasmic dynein heavy chain is required for oscillatory nuclear movement of meiotic prophase and efficient meiotic recombination in fission yeast. J. Cell Biol. *145*, 1233–1249.

Yamashita, A., and Yamamoto, M. (2006). Fission yeast Num1p is a cortical factor anchoring dynein and is essential for the horse-tail nuclear movement during meiotic prophase. Genetics *173*, 1187–1196.

Yokobayashi, S., and Watanabe, Y. (2005). The kinetochore protein Moa1 enables cohesion-mediated monopolar attachment at meiosis I. Cell *123*, 803–817.